DOI: 10.1002/ejic.200900375

A New Manganese Coordination Polymer Containing 1,2,4-Benzenetricarboxylic Acid

Huey-Ting Chung,[a] Hui-Lien Tsai,[b] En-Che Yang,[a] Po-Hsiu Chien,[a] Chia-Chien Peng,[a] Yun-Chieh Huang,[a] and Yen-Hsiang Liu*[a]

Keywords: Manganese / Metal-organic frameworks / Solvothermal synthesis / Crystal engineering / Magnetic properties

The reaction of an unsymmetrical ligand, namely 1,2,4-benzenetricarboxylic acid (H_3btc), under pH-controlled hydrothermal conditions with a manganese salt leads to the three-dimensional coordination polymer $\{Mn(H_2O)[C_6H_3(CO_2)_2(CO_2H)]\cdot(H_2O)\}_n$ (**FJU-2**). Potassium hydroxide is used as a control agent to modulate the degree of deprotonation of the unsymmetrical H_3btc ligand during the hydrothermal reaction, which is essential for the synthesis of the resulting product. The product was characterised by elemental, single-crystal and powder X-ray analyses. The structure of **FJU-2** consists of carboxylate- and water-bridged manganese cluster chains which are further cross-connected by the phenyl spacer into a three-dimensional neutral framework. Guest water molecules reside in an elliptically shaped, one-dimensional channel. There are strong hydrogen-bonding interactions between the guest water molecules and host framework that prevent the release of the guest water molecules at lower temperatures, as indicated by the thermogravimetric analysis. The magnetic study shows an antiferromagnetic coupling for **FJU-2**.

Introduction

The self-assembly process driven by metal-carboxylate coordination has been exploited as a useful tool for the crystal-engineering design of coordination polymers with extended network structures.[1–8] Multi-fold benefits are derived from such coordination chemistry. The use of linear,[1] triangular[2] and tetrahedral[3] phenylpolycarboxylic acids as bridging spacer/linkers with a symmetrical bonding geometry, for example, favours the design of framework solids with a systematically tuneable framework topology and cavity properties. On the other hand, unsymmetrical phenylpolycarboxylic acids, such as biphenyl-3,4′,5-tricarboxylic acid, which have different binding motifs on each side of the organic linker, can extend the diversity of the resulting network topologies.[4] The appropriate choice of phenylpolycarboxylic acid linker may also produce a high channel surface area for gas adsorption.[5] Diverse metal-carboxylate coordination and bridging modes facilitate the formation of polynuclear core motifs, such as clusters and chains, which favourably affect network topology diversity, the magnitude and nature of the magnetic coupling interaction between carboxylate-bridged paramagnetic metal centres, and provide high structural stability.[6,7]

We and co-workers have recently been interested in the crystal engineering design of metal-polycarboxylate coordination polymers using 1,2,4,5-benzenetetracarboxylic acid as the bridging ligand and in investigating the influence of the reaction conditions (for example, duration of time of self-assembly, cation templates and ion-exchange effects) on the resulting network topologies.[8] In this work, we focus our attention on the use of a simple, unsymmetrical phenylpolycarboxylic acid, namely 1,2,4-benzenetricarboxylic acid, as the bridging ligand in the synthesis of the three-dimensional coordination polymer $\{Mn(H_2O)[C_6H_3(CO_2)_2(CO_2H)]\cdot(H_2O)\}_n$ (**FJU-2**) under hydrothermal conditions. Unlike the more symmetrical 1,2,4,5-benzenetetracarboxylate ligand, this strategy relies on the fact that the distinct coordination environments of the carboxylate groups at the 1-, 2- and 4-positions of the benzene ring enrich the structural diversity of the resulting coordination networks. Furthermore, a partially deprotonated 1,2,4-benzenetricarboxylic acid (H_3btc), generated by appropriate control of the reaction pH, allows this ligand to serve as both a network linker and a hydrogen bonding donor–acceptor and π–π interaction site. Moreover, the extent of deprotonation of the H_3btc ligand provides more sophisticated coordination environments with metal ions during the self-assembly process, thereby extending the possibilities of constructing new network structures. The thermal and magnetic properties of **FJU-2** are also investigated.

[a] Department of Chemistry, Fu Jen Catholic University, Taipei 24205, Taiwan
Fax: +886-2-2902-3209
E-mail: chem2022@mails.fju.edu.tw
[b] Department of Chemistry, National Cheng Kung University, Tainan, Taiwan
Supporting information for this article is available on the WWW under http://dx.doi.org/10.1002/ejic.200900375 or from the author.

Results and Discussion

Synthesis

The complex **FJU-2** was successfully synthesised under pH-controlled hydrothermal conditions by treating the manganese salt $MnCl_2 \cdot 4H_2O$ with H_3btc. The phase-purity of the bulk materials was independently confirmed by elemental microanalysis, PXRD and TGA. Energy-dispersive X-ray analysis confirmed the presence of manganese. **FJU-2** was characterised as having the formula $\{Mn(H_2O)[C_6H_3(CO_2)_2(CO_2H)] \cdot H_2O\}_n$ on the basis of single-crystal X-ray diffraction and elemental analysis results. It is noteworthy that the use of an alkali metal hydroxide to control the pH and produce partially deprotonated H_3btc ligands is essential for the synthesis of **FJU-2** (Scheme 1).

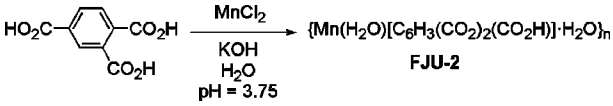

Scheme 1. A 3D manganese coordination polymer is assembled under pH-controlled hydrothermal conditions.

Structural Description

The solid-state structure of **FJU-2** was revealed by single-crystal X-ray diffraction analysis. The crystallographic asymmetric unit contains one Mn^{II} ion, one btc ligand, one coordinated water molecule and one guest water molecule (Figure 1).

Only two out of the three carboxyl groups of the H_3btc ligand are deprotonated to achieve charge neutrality with the Mn^{II} ion. This was confirmed by the assignment of the hydrogen atom of the carboxyl group from the difference Fourier map and the observation of asymmetrical carbon–oxygen bond lengths for the carboxyl group [C(9)–O(5) 1.306(3) and C(9)–O(6) 1.229(3) Å]. The other two carboxylate groups of the $Hbtc^{2-}$ ligand, have more symmetrical carbon–oxygen bond lengths ranging from 1.241(3) to 1.271(3) Å. (Table 1) As a result, the $Hbtc^{2-}$ ligand engages in three distinct types of coordination with the manganese ions (Scheme 2).

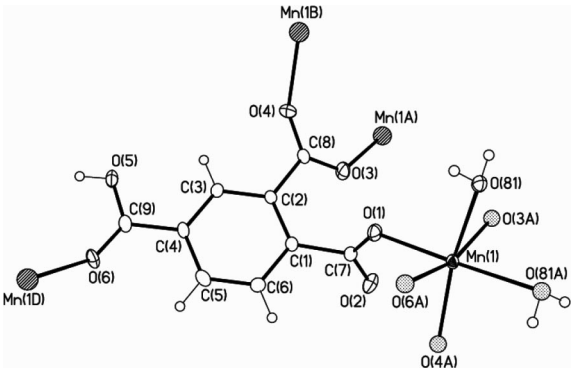

Figure 1. Numbering scheme and the metal–ligand coordination environment of **FJU-2**. The guest water molecule has been omitted for clarity.

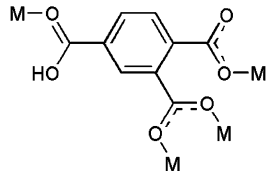

Scheme 2. The coordination mode of the $Hbtc^{2-}$ ligand.

The manganese ion adopts an octahedral coordination environment and is surrounded by two coordinated water molecules and four oxygen atoms from both carboxyl and carboxylate groups. As shown in Figure 2, two octahedral Mn centres are bridged by two water molecules to form edge-shared octahedra, which are further linked by double carboxylate bridges to form infinite one-dimensional metallic chains along the (100) direction.

The manganese chains can be considered to be secondary building blocks and are further cross-linked by the phenyl spacer of the $Hbtc^{2-}$ anions to form a three-dimensional framework, as illustrated in Figure 3. Elliptically shaped

Table 1. Selected bond lengths [Å] and angles [°] for **FJU-2**.[a]

Mn(1)–O(3)#1	2.0936(16)	O(1)–C(7)	1.271(2)
Mn(1)–O(4)#2	2.0938(16)	O(2)–C(7)	1.241(3)
Mn(1)–O(1)	2.1522(15)	O(3)–C(8)	1.255(3)
Mn(1)–O(6)#3	2.2185(16)	O(4)–C(8)	1.251(3)
Mn(1)–O(81)	2.3378(15)	O(5)–C(9)	1.306(3)
		O(6)–C(9)	1.229(3)
O(3)#1–Mn(1)–O(4)#2	112.35(7)	O(4)#2–Mn(1)–O(81)#4	89.08(6)
O(3)#1–Mn(1)–O(1)	89.78(6)	O(6)#3–Mn(1)–O(81)#4	89.70(6)
O(4)#2–Mn(1)–O(1)	94.14(6)	O(3)#1–Mn(1)–O(81)	85.37(6)
O(4)#2–Mn(1)–O(6)#3	85.89(7)	O(1)–Mn(1)–O(81)	100.84(6)
O(1)–Mn(1)–O(6)#3	86.71(6)	O(6)#3–Mn(1)–O(81)	77.64(6)
O(3)#1–Mn(1)–O(81)#4	92.56(6)	O(81)#4–Mn(1)–O(81)	74.95(6)

[a] Symmetry transformations used to generate equivalent atoms: #1 $-x + 1, -y, -z+1$; #2 $x, y + 1, z$; #3 $-x + 1, -y, -z$; #4 $-x + 2, -y + 1, -z + 1$.

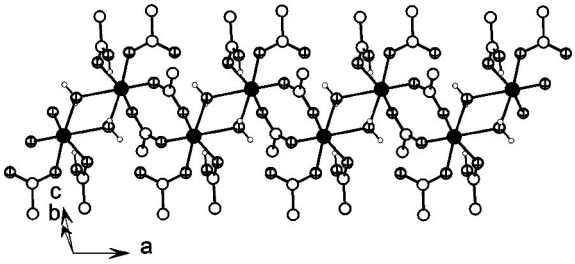

Figure 2. A view of the one-dimensional manganese chain in **FJU-2**.

channels, which contain uncoordinated water molecules, are observed along the (100) direction. A water- and carboxylate-bridged manganese coordination polymer with a stair-like network structure, $[Mn_2(H_2O)_4(cda)\cdot 4H_2O]_n$ (chelidamic acid, $cdaH_2$), has recently been reported.[9]

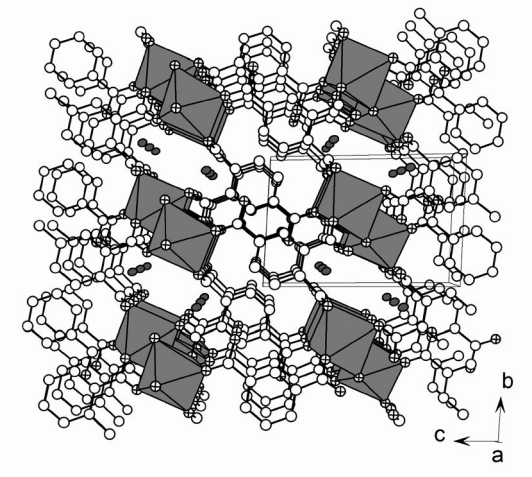

Figure 3. A perspective view of the 3D framework of **FJU-2** along the (100) direction. Grey ellipsoids: guest water molecules; grey octahedra: $[MnO_6]$.

It is noteworthy that four strong O–H···O-type hydrogen-bonding interactions are observed between the guest water molecules and the surrounding host framework (Table 2), including hydrogen atoms of the bridging water molecule, hydrogen atoms of the carboxyl groups and oxygen atoms of two carboxylate ligands that interact in a tetrahedral arrangement (Figure 4).

Table 2. Hydrogen bonds for **FJU-2** [Å and °].

D–H···A	*d*(D–H)	*d*(H···A)	*d*(D···A)	<DHA
O(5)–H(15)···O(91)	0.83	1.79	2.611(2)	174
O(81)–H(81A)···O(91)	0.85	1.85	2.695(2)	179
O(91)–H(91A)···O(1)	0.78	1.93	2.707(2)	174
O(91)–H(91B)···O(2)	0.88	1.76	2.645(2)	177

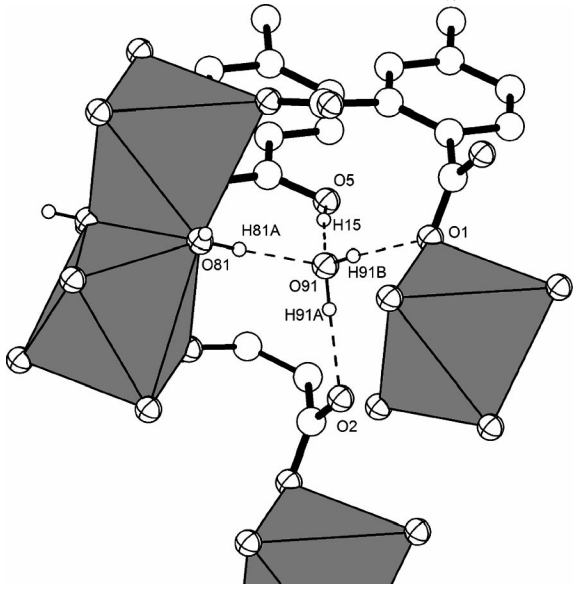

Figure 4. Part of the packing diagram showing strong hydrogen-bonding interactions between the guest water molecule and the host.

Thermal Stability Analysis and Host–Guest Interactions

The thermal stability of the solid framework of **FJU-2** was analysed by both thermogravimetric (TG) analysis and variable-temperature powder X-ray diffraction (VT-PXRD) analysis. The result of the TG analysis of **FJU-2** is illustrated in Figure 5 and is consistent with the crystallographic observations.

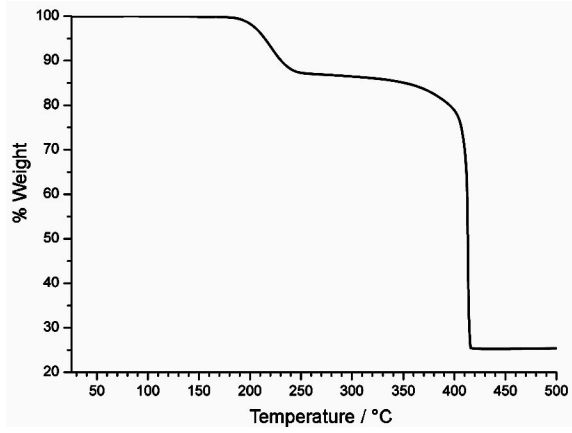

Figure 5. The thermogravimetric diagram of **FJU-2**.

The TG trace of **FJU-2** shows no weight loss up to a temperature of 190 °C due to the very strong hydrogen-bonding interactions between the host framework and the nonligated guest water molecules. The continuous release of guest water molecules, as well as the decomposition of bridging water molecules, occurs between 190 and 250 °C (total weight loss: 12.7%). This weight loss (calcd. 12.5%) corresponds to one nonligated water molecule and one

bridging water molecule per formula unit. To further test the thermal stability of **FJU-2**, a freshly ground sample was subjected to powder X-ray diffraction analyses at 80, 160 and 250 °C. The major peaks in the VT-PXRD patterns of the heated sample show no change in the diffraction peak position at either 80 or 160 °C with respect to as-synthesised **FJU-2** at room temperature.[10] Upon removal of the nonligated and bridging water molecules at 250 °C, **FJU-2** loses its original framework topology, as indicated by the distinct peak positions in the diffraction patterns (Figure 6). The results of the VT-PXRD analyses are consistent with the crystallographic observations. The strong host–guest hydrogen-bonding interactions observed in **FJU-2** prevent the release of guest water molecules at lower temperatures and loss of both nonligated and bridging water molecules at high temperatures, thereby altering the framework architecture of **FJU-2**.

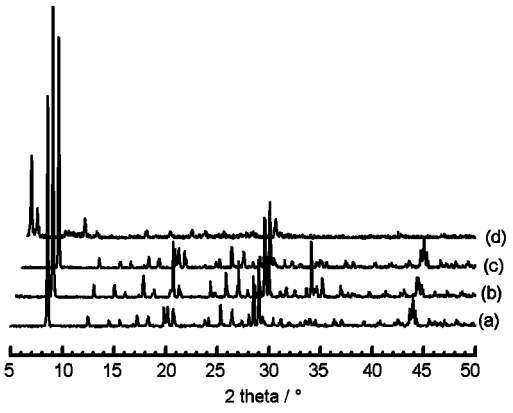

Figure 6. Variable-temperature powder X-ray diffraction diagrams of **FJU-2** at (a) room temperature, (b) 80 °C, (c) 160 °C, (d) 250 °C.

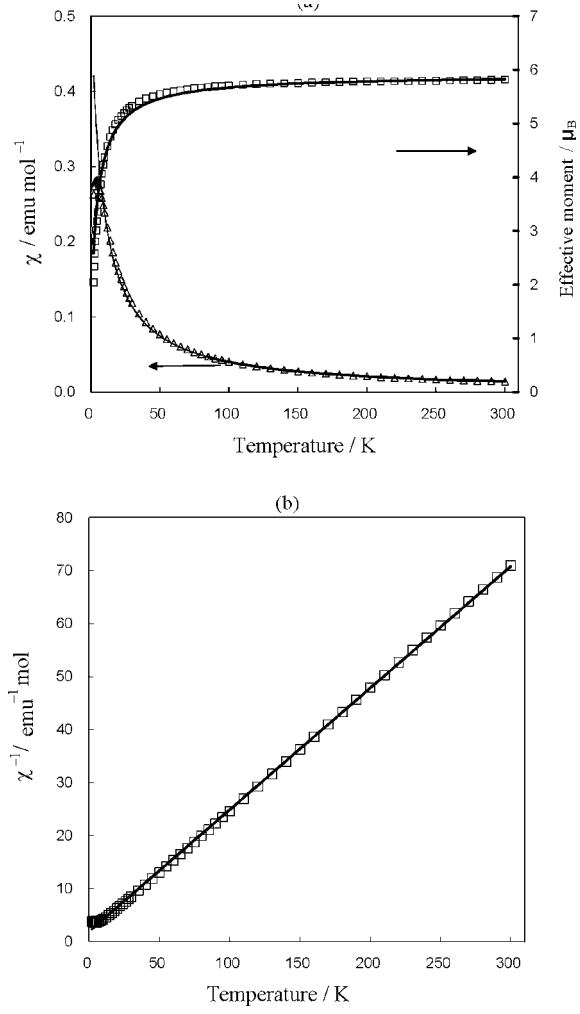

Figure 7. (a) Plots of χ_M-T (left) and μ_{eff}-T (right) for a polycrystalline sample of **FJU-2**. χ_M is the molar susceptibility, μ_{eff} is the effective magnetic moment. Data were collected in an applied field of 1000 G. (b) Plot of $1/\chi_M$-T. The solid line is estimated from the Curie–Weiss law.

Magnetism

Variable-temperature magnetic susceptibility measurements of **FJU-2** were carried out in a 1000 G magnetic field from 2 to 300 K. Figure 7 shows the χ_M-T and μ_{eff}-T plots of this sample. The μ_{eff} value is 5.82 μ_B at 300 K, and remains roughly constant at 5.67 μ_B down to 80 K. It then slowly decreases to 5.07 μ_B at 20 K and drops sharply to 2.05 μ_B at 2 K. The spin-only value of μ_{eff} for a non-interacting Mn^{II} cation is about 5.92 μ_B, which agrees with the experimental value of 5.80 μ_B at 300 K. The decrease in μ_{eff} with decreasing temperature indicates an antiferromagnetic coupling in this complex. The susceptibility data were further studied in the form of a $1/\chi_M$-T plot. Figure 7 (b) shows the fit to the Curie–Weiss law [$1/\chi_M = (T - \theta)/C$, solid line], which gives a Curie constant, C, of 4.36 $cm^3 K mol^{-1}$ and θ = –8.37 K, thereby confirming the antiferromagnetic interactions in this complex. The parameters obtained from the Curie–Weiss law allowed an estimation of the χ_M-T and μ_{eff}-T curves (solid lines in part a of Figure 7), which are consistent with the experimental data.

Conclusions

We have succeeded in creating a new 1,2,4-benzenetricarboxylate-based coordination polymer by using potassium hydroxide as the deprotonating agent. The hydrothermal synthesis, crystal structure and magnetic properties of this polymer have been described. The degree of deprotonation of 1,2,4-benzenetricarboxylic acid affects both the metal–ligand coordination modes and the resulting network topology and also influences the interactions between the guest molecules and the host framework. Further work using other base systems such as organic amines is well under way to probe the structural modulation of different network structures and their host–guest chemistry.

Experimental Section

Materials and Instrumentations: All reagents and solvents were commercially available and were used as supplied without further purification. Elemental analyses were performed with a Perkin–El-

mer 2400 elemental analyzer. Thermogravimetric analyses (TGA) were performed with a Perkin–Elmer TGA-7 TG analyzer at a heating rate of 5 °C/min under nitrogen. Powder X-ray diffraction (PXRD) measurements were performed in step mode with a fixed time of 10 s and a step size of 0.02° in θ on a Siemens ^{d}-5000 diffractometer at 40 kV, 30 mA with Cu-K_α radiation (λ = 1.5406 Å). Variable-temperature dc magnetic susceptibility data were collected for polycrystalline samples of **FJU-2** in an applied field of 1.0 kG in the temperature range 2.0–300.0 K, and were measured using a SQUID magnetometer (Quantum Design, MPMS-7). The samples were embedded in eicosane wax to prevent any torquing of the sample in the magnetic field. Pascal's constants[11] were used to estimate the diamagnetic corrections.

Synthesis of $\{Mn(H_2O)[C_6H_3(CO_2)_2(CO_2H)]\cdot(H_2O)\}_n$ (FJU-2): H_3btc (1.01 mmol, 211.5 mg) was dissolved in 10 mL of water and 4 M KOH solution was then added dropwise to adjust the pH of the solution to about 3.75. $MnCl_2\cdot 4H_2O$ (1.58 mmol, 311.9 mg) was added to this aqueous solution and the mixture stirred for 30 min at room temperature. It was then sealed in a Teflon®-lined stainless-steel vessel and heated at 110 °C for 72 h under hydrothermal conditions. After cooling to ambient temperature, the crystalline solid product was washed with distilled water and isolated by suction filtration. The final product contained a single phase of plate-like crystals of **1** (202.2 mg) in a yield of 66.9% based on H_3btc. A powder X-ray diffraction pattern of the bulk sample compared well with the pattern simulated from single-crystal data. Elemental analysis: calcd. C 36.14, H 2.70; found C 35.98, H 2.77.

X-ray Crystallography: A suitable crystal was mounted on a thin glass fibre for structure identification. Intensity data were collected on a Siemens P4 diffractometer in the θ range 1–30° using graphite-monochromated Mo-K_α radiation (λ = 0.71073 Å) at 298 K. Crystal unit-cell parameters were obtained by centring 32 reflections with θ values of between 5° and 13°, and was determined to be triclinic with space group $P\bar{1}$. Intensity data were corrected for background, Lorentz, polarisation and absorption effects. A trial structure model was obtained by direct methods with successive interpretation of difference Fourier maps, and was refined by full-matrix least-squares using SHELXL97.[12] All non-hydrogen atoms were refined anisotropically. The hydrogen atoms of the carboxyl group and water molecules were located from the difference Fourier maps and refined as riding atoms with a common fixed isotropic displacement. The C–H hydrogen atoms were placed in idealised positions and refined as riding atoms with a common fixed isotropic displacement parameter. Crystal data and experimental details are given in Table 3.

CCDC-727449 contains the supplementary crystallographic data for this paper. These data can be obtained free of charge from The Cambridge Crystallographic Data Centre via www.ccdc.cam.ac.uk/data_request/cif.

Supporting Information (see also the footnote on the first page of this article): Powder X-ray diffraction diagram of the heated sample of **FJU-2** at 190 °C.

Table 3. Crystallographic data for **FJU-2**.

Formula	$MnC_9H_8O_8$
M	299.09
Temperature [K]	298(2)
Crystal system	triclinic
Space group	$P\bar{1}$
a [Å]	6.4084(6)
b [Å]	7.355(2)
c [Å]	10.882(3)
α [°]	92.202(2)
β [°]	100.894(7)
γ [°]	100.013(6)
V [Å^3]	494.7(2)
Z	2
ρ [g cm^{-3}]	2.008
μ [mm^{-1}]	1.370
F(000)	302
Crystal size [mm^3]	0.5 × 0.25 × 0.15
Reflections collected/unique	3011/2382
R(int)	0.0508
GOF	1.056
$R1$,[a] $wR2$[b] [$I > 2\sigma(I)$]	0.0317, 0.0747
$R1$,[a] $wR2$[b] (all data)	0.0409, 0.0796
Largest diff. peak and hole [e Å^{-3}]	0.443/–0.362

[a] $R1 = \Sigma||F_o| - |F_c||$. [b] $wR1 = \{\Sigma[w(F_o^2 - F_c^2)]/\Sigma[w(F_o^2)^2]\}^{1/2}$.

Acknowledgments

This work was supported by the National Science Council and Fu Jen Catholic University, Taiwan.

[1] a) S. A. Bourne, J. Lu, A. Mondal, B. Moulton, M. J. Zaworotko, *Angew. Chem. Int. Ed.* **2001**, *40*, 2111; b) M. Eddaoudi, J. Kim, N. Rosi, D. Vodak, J. Wachter, M. O'Keefe, O. M. Yaghi, *Science* **2002**, *295*, 469; c) F. Salles, A. Ghoufi, G. Maurin, R. G. Bell, C. Mellot-Draznieks, G. Férey, *Angew. Chem. Int. Ed.* **2008**, *47*, 8487.

[2] a) S. S.-Y. Chui, S. M.-F. Lo, J. P. H. Charmant, A. G. Orpen, I. D. Williams, *Science* **1999**, *283*, 1148; b) H. K. Chae, D. Y. Siberio-Perez, J. Kim, Y. Go, M. Eddaoudi, A. J. Matzger, M. O'Keeffe, O. M. Yaghi, *Nature* **2004**, *427*, 523.

[3] B. L. Chen, M. Eddaoudi, T. M. Reineke, J. W. Kampf, M. O'Keeffe, O. M. Yaghi, *J. Am. Chem. Soc.* **2000**, *122*, 11559.

[4] A. G. Wong-Foy, O. Lebel, A. J. Matzger, *J. Am. Chem. Soc.* **2007**, *129*, 15740.

[5] a) M. Latroche, S. Surblé, C. Serre, C. Mellot-Draznieks, P. L. Llewellyn, J.-H. Lee, J.-S. Chang, S. H. Jhung, G. Férey, *Angew. Chem. Int. Ed.* **2006**, *45*, 8227; b) A. G. Wong-Foy, A. J. Matzger, O. M. Yaghi, *J. Am. Chem. Soc.* **2006**, *128*, 3494.

[6] a) C. N. R. Rao, S. Natarajan, R. Vaidhyanathan, *Angew. Chem. Int. Ed.* **2004**, *43*, 1466; b) Y.-Z. Zheng, Y.-B. Zhang, M.-L. Tong, W. Xue, X.-M. Chen, *Dalton Trans.* **2009**, 1396; c) L. Hou, J.-P. Zhang, X.-M. Chen, S. W. Ng, *Chem. Commun.* **2008**, 4019; d) J. Yang, J.-F. Ma, Y.-Y. Liu, S. R. Batten, *CrystEngComm* **2009**, *11*, 151; e) L.-F. Ma, L.-Y. Wang, Y.-Y. Wang, M. Du, J.-G. Wang, *CrystEngComm* **2009**, *11*, 109; f) H. Chun, H. Jung, *Inorg. Chem.* **2009**, *48*, 417; g) S. K. Ghosh, W. Kaneko, D. Kiriya, M. Ohba, S. Kitagawa, *Angew. Chem. Int. Ed.* **2008**, *47*, 8843; h) X.-J. Li, X.-Y. Wang, S. Gao, R. Cao, *Inorg. Chem.* **2006**, *45*, 1508; i) J. Chen, M. Ohba, D. Zhao, W. Kaneko, S. Kitagawa, *Cryst. Growth Des.* **2006**, *6*, 664.

[7] a) Q.-R. Fang, G.-S. Zhu, Z. Jin, M. Xue, X. Wei, D.-J. Wang, S.-L. Qiu, *Angew. Chem. Int. Ed.* **2006**, *45*, 6126; b) K. Barthelet, K. Adil, F. Millange, C. Serre, D. Riou, G. Ferey, *J. Mater. Chem.* **2003**, *13*, 2208; c) F. Luo, S. R. Batten, Y. Che, J.-M. Zheng, *Chem. Eur. J.* **2007**, *13*, 4948; d) L.-F. Ma, L.-Y. Wang, Y.-Y. Wang, M. Du, J.-G. Wang, *CrystEngComm* **2009**, *11*, 109; e) M. Xue, G. Zhu, Y. Li, X. Zhao, Z. Jin, E. Kang, S. Qiu, *Cryst. Growth Des.* **2008**, *8*, 2478; f) F. Luo, Y.-T. Yang, Y.-X. Che, J.-M. Zheng, *CrystEngComm* **2008**, *10*, 1613; g) Y. Liu, J. F. Eubank, A. J. Cairns, J. Eckert, V. C. Kravtsov, R. Luebke, M. Eddaoudi, *Angew. Chem. Int. Ed.* **2007**, *46*, 3278; h) Q.-R. Fang, G.-S. Zhu, Z. Jin, M. Xue, X. Wei, D.-J. Wang, S.-L. Qiu, *Cryst. Growth Des.* **2007**, *7*, 1035; i) Q.-R. Fang, G.-S. Zhu, Z. Jin, M. Xue, X. Wei, D.-J. Wang, Shi-Lun Qiu, *Angew. Chem. Int. Ed.* **2006**, *45*, 6126; j) Q.-R. Fang, G.-S. Zhu, M. Xue, Q.-L. Zhang, J.-Y. Sun, X.-D. Guo, S.-L. Qiu, S.-T. Xu, P. Wang, D.-J. Wang, Y. Wei, *Chem. Eur. J.* **2006**, *12*, 3754;

k) D. Dobrzyńska, L. B. Jerzykiewicz, J. Jezierska, M. Duczmal, *Cryst. Growth Des.* **2005**, *5*, 1945.
[8] a) Y.-H. Liu, M.-T. Ding, *Acta Crystallogr., Sect. E* **2007**, *63*, m1828; b) J.-Y. Wu, S.-L. Yang, T.-T. Luo, Y.-H. Liu, Y.-W. Cheng, Y.-F. Chen, Y.-S. Wen, L.-G. Lin, K.-L. Lu, *Chem. Eur. J.* **2008**, *14*, 7136; c) J.-Y. Wu, M.-T. Ding, Y.-S. Wen, Y.-H. Liu, Kuang-Lieh Lu, *Chem. Eur. J.* **2009**, *15*, 3604.
[9] S. K. Ghosh, J. Ribas, M. S. El Fallah, P. K. Bharadwaj, *Inorg. Chem.* **2005**, *44*, 3856.
[10] The 2θ values [°] of the major diffraction peaks of the as-synthesized sample of **FJU-2** are: 8.58, 12.50, 14.43, 15.58, 17.27, 18.31, 19.87, 20.22, 20.77, 20.89, 24.17, 25.34, 26.48, 28.06, 28.51, 29.03, 29.40, 30.45, 31.19, 36.35, 43.63, 43.96, 44.22, 44.33, 47.01.
[11] *Theory and Application of Molecular Paramagnetism* (Eds.: E. A. Boudreaux, L. N. Mulay), John Wiley & Sons, New York, **1976**.
[12] G. M. Sheldrick, *SHELXL97*, University of Göttingen, Germany, **1997**.

Received: April 25, 2009
Published Online: July 15, 2009

